Chapter 14: The Mega-provincial cratering of North America

Abstract

Structure of South Pole-Aitken Basin and Mare Imbrium are studied to find characteristics of larger craters on the moon. The characteristics are related back to large circular patterns on the earth that characterized possible cratering structures across and adjacent to North America. Six of the largest craters and one smaller one suggest a sequence of occurrence that relates to the lithology. The Keys, Bermuda, Foxe, Maka Luta, Tatanka, Alvord, and Caribou craters have interactive energy signatures that relate to each other and to the Ipojuca, Irminger, Tasman Sea, and Bahia Grande impactors which were occurring in the same timeframe.

Introduction

What were the first craters in North America? We will assume they were also the largest craters. If they were not, the smaller craters would have become buried in the big one, so we will assume we are looking for big craters. To understand the evidence for big craters, let's look at the two largest craters on the Moon: South Pole-Aitken basin and Mara Imbrium.

South Pole-Aitken Basin

Using the method laid out in Chapter 11, Figure 14.1 compares the data maps of the area. The GRAIL gravity map (A) does not show a prominent Mascon, like we will see in Mare Imbrium and the smaller craters: Apollo (A), Leibnitz (L), Poincaré (P). Crustal Thickness (C) also does not show a well-defined area of thinner crust. James et al (2019) does mention a denser gravity just in the center, but they fail to refer to it as a mascon. Figure 14.2 shows a more detailed view of the center of the crater with the thinnest crust, and that image shows a reddish center in each of the small craters, showing the denser masses may not penetrate to the bottom of the mantle uplift. This shows mascons have a bottom and may only penetrate proportional to their diameter

Figure 14.3 shows a section through the 2500+ km diameter crater using the more detailed data set with the northern and southern most point of my OCR-ring indicated, and it does exhibit the raised mantle associated with the other larger craters Figures 11.3, 11.5, 11.8. The dimmer indication of greater mass and the yellow masses in Apollo and Poincaré craters, and the lacking of any indication of mascon in Leibnitz, and Schrödinger suggest the origin of mascons are proportional and limited by the occurrence of other energy signatures in the same area to add to the upthrust of a mascon as recognized in Chapter 10A.

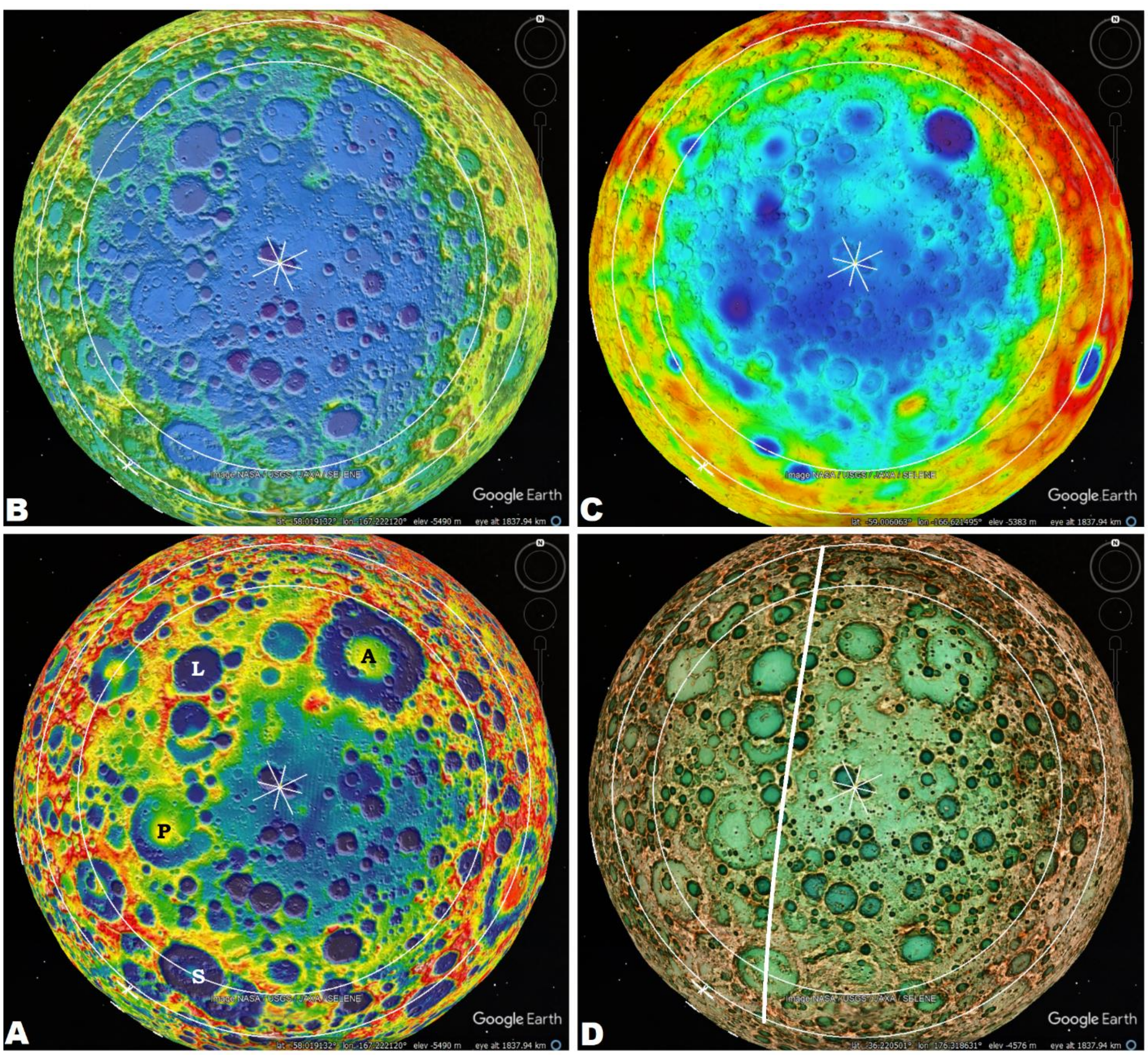

In the Red Relief map (D) the white arced line indicates the up-side of a CGRS possibly from Grimaldi Crater. The prominence of multiple linears/CGRS from multiple sources within South Pole-Aitken Basin suggest there is a time component to the expression of mascons, and if this basin was an early crater, there may not have already been energy signatures from other cratering events to be expressed in its crater floor's rebound (Figure 12.17G)

Figure 14.1: Four views of South Pole-Aitken in the southern farside of the Moon. (A) GRAIL gravity, (B) Topography, (C) Crustal Thickness (Thinnest is blue and thickest is red), and (D) Red Relief. Labeled small crater are Apollo (A), Leibnitz (L), Poincaré (P), and Schrödinger (S).

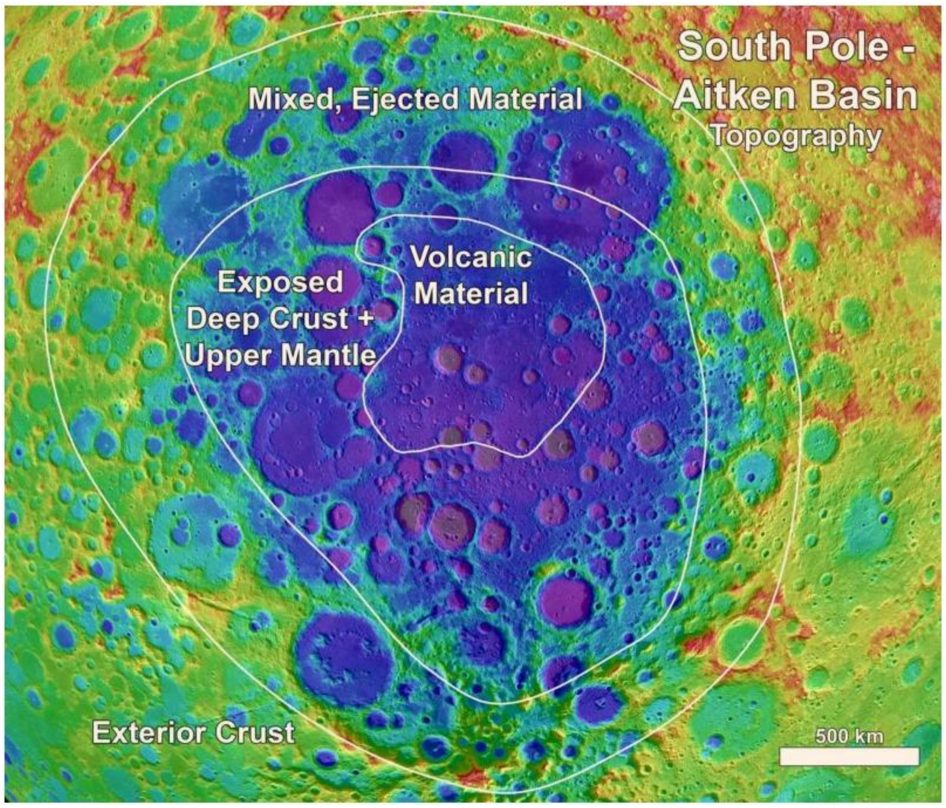

Figure 14.2: High resolution detail of South Pole-Aitken Basin's center showing redder centers in many of the smallest craters. (Image from Goddard Space Center.)

Figure 14.3: Diagrammatic section from north to south for South Pole-Aitken Basin, assembled from GRAIL data. (Redrawn from James et al 2019.)

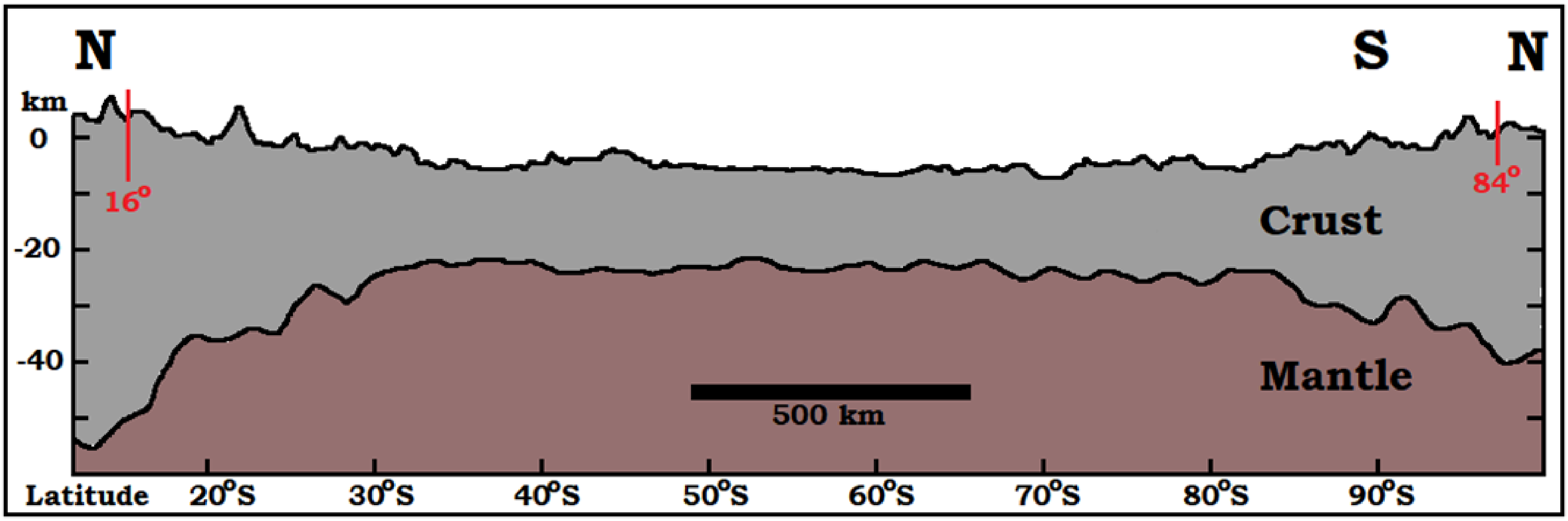

Mare Imbrium

Mare Imbrium is the largest crater on the nearside of the moon and would be a good example of recognizing large earth craters. Figure 15.4 compares the crater data on the four different maps. The thinnest crust (image C), blue, and the inner rim of mountains on the topography view (image B) coincide with the red of the mascon on the gravity map (image A). This defines the inner ring, or Open-ring as I have designated it. Although the Open-ring cannot be seen in topography, it is lying just outside the mascon and area of thinnest crust. Looking again at the topography map (image B) the next circle out is the most distinct ring and I will designate it the (Original Crater Rim) OCR-ring.

Comparing the section between the Open-ring and the OCR-ring on the Red Relief map (image D), the northeast two-thirds is the roughest terrane, but it is the bluest portion, lowest gravity, in the GRAIL (image A). Since mountain building on the moon is a direct result of cratering, this is a consistent correlation between mountains location and low gravity (blue areas) outside of the dense center of the mascon. As the Rocky Mountains are the most densely occurring mountain area in North America, if cratering is responsible for the terrane, we would expect it to show heavily blue in gravity. By contrast, the lowest area in the South Pole-Aitken Basin is also the bluest, lowest gravity, area.

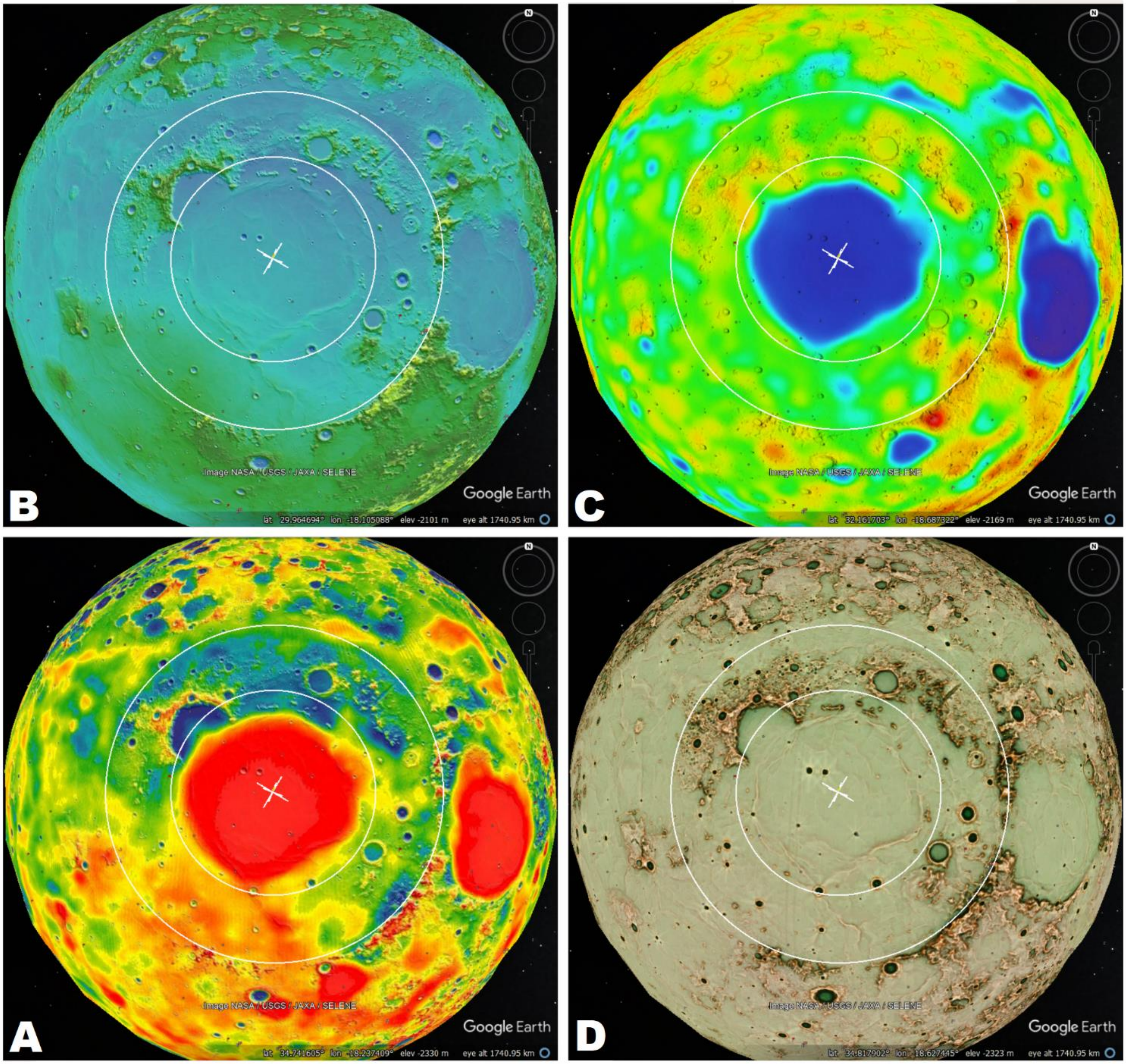

Figure 14.4: Four views of Mare Imbrium in (A) GRAIL gravity, (B) Topography, (C) Crustal Thickness (Thinnest is blue and thickest is red), and (D) Red Relief.

The blue area is blue because it has experienced adiabatic shattering and scattering of its lithology and is composed of a less dense lithology (Chapter 6) which may be related to more pore-space or less dense mineralogy. But whatever its cause, it lies within the cratering bowl (Figure 14.4 compared with Figure 12.17G).

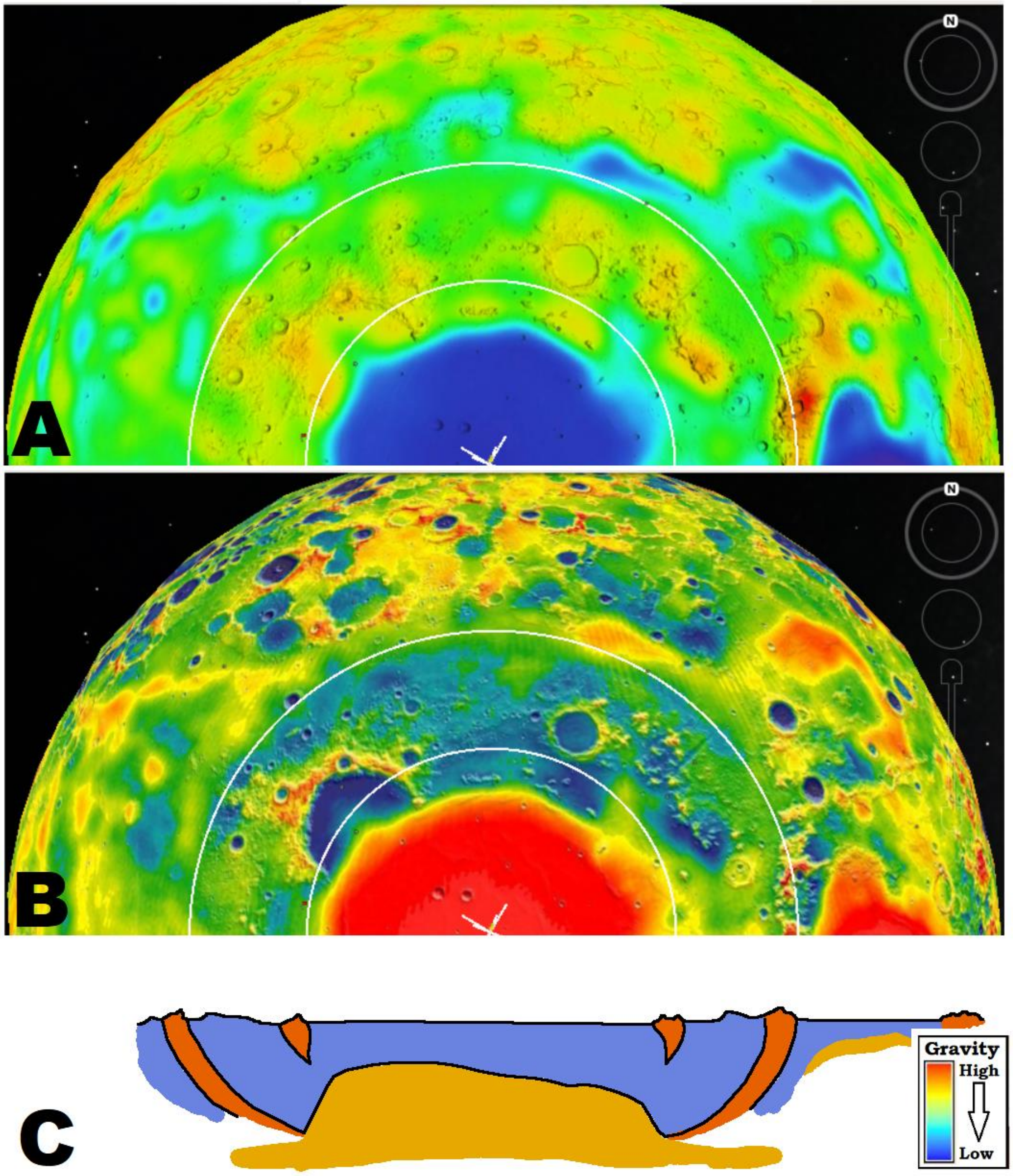

Figure 14.5: Mare Imbrium in cross section (C) derived from comparing the thinnest crust (A) with GRAIL gravity (B), and recognizing the blue/low gravity basin fill.

Figure 14.6A shows the location of ripples and shallow depression in the lava on the surface within the Open-ring. It is proposed that the prominent ripples were formed around the rim of individual lava fields or flows (Zhang et al 2015). As the lava ripples can be seen to rim circular craters, recognized in the darker depressions (Figure 14.3B), but the most prominently ridges lie outside the mascon. The relationship between the smaller craters and the ripples show the lava was responding to smaller impactors which were falling into it, and CGRS that were crossing it during the time it was cooling. As these ripples predominantly lie outside of the mascon, I propose these ridges represent an excess of lava within that area produced when the crater floor rebounded, Figure 12.17G. This time frame would make the arrival of the lava and additional smaller craters, with the CGRS, all within the crater forming process. Minutes or hours after impact, much earlier than these arrivals are generally thought to have occurred.

Mare Imbrium Regolith

[Zhang et al 2019 provides the following summary of the sub-surface structure of the Imbrium basin, paraphrased here for length.] Apollo mission to the moon was able to directly determine the regolith reached at least ~2.8 m using a drilling core. Using seismic data they were able to estimate depths of 4.4, 3.7, 8.5, 4.4, 12.2, and 4.0 m at the Apollo 11, 12, 14, 15, 16, and 17 landing sites, respectively. The Japanese mission Kaguya, using laser altimeter, showed variation from 5-20 m, using a two-layer regolith model. China’s Chang’E-1 lunar mission using multi-channel radiometer estimated 4.5 m thickness within the maria and 7.6 m in the farside highlands. When the Chang’E-1 landed in the northwest sector of Mare Imbrium, the dual-frequency Lunar Penetrating Radar aboard the Yutu Rover identified nine subsurface layers in a depth of ~360 m. Hard layers, possibly basalts, were located at 195, 215, and 345 m.

The Yutu Rover tracing a path 114 m long, and imaged in greater detail down to ~14 m along that path. Four distinct layers of regolith were discerned. (I) a consistent pebble layer covering the entire surface ~0.5 m thick. Zhang et al labeled it as “strong degree of weathering.” (II) A fine granular layer filling up to 3 m irregularities in its bottom surface. They labelled it as “weak degree of weathering." (III) A finer breccia ~2.0 m thick, roughly parallel on its two surfaces. They labeled it as "strong degree of weathering." (IV) A coarse breccia up to 2 m in diameter and piled up, laying over a hard surface. They identified it as "weakly weathered" (page 159).

I would interpret the four layers as the large breccia fallback from an impact distributed originally by force propelled particle rushing out of the cratering event. And, the degree of "weathering" a response to the amount of heat it was subject to while airborne. This large breccia was immediately buried by the smaller breccia, which was immediately buried by a mixed granular material from the bursting of the adiabatic envelope. This mixed granular material was winnowed like a "desert pavement" by strong expulsion forces until only the larger pebbles remained. The depth of this layer, ~0.5 m, testifies to the strength of these winds. All four of these layers built up on a hard surface compressed and compacted by the original shock wave of the crater's excavation.

Figure 14.8: Ridges in the Lava just inside the Open Ring suggest lava was moved/lifted while cooling into position. As these ridges lie over the blue area in GRAIL, this raising would correspond with the rising of the Mascon. This recognizes that the lava emplacement was part of the cratering process, not a later one. This directly suggest LIPs on earth are ALSO part of the cratering process, within the SAME time frame, not a later occurrence. A number of larger midsize craters fill the mare and make sinus like lobes beyond the mascon. Even Sinus Iridum blue circle in Figure 14.10, has a "nipple" of added red in the mascon. This means the mascon was not finally formed until the Iridum impactor had arrived. Another indicator of the short timescale involved.

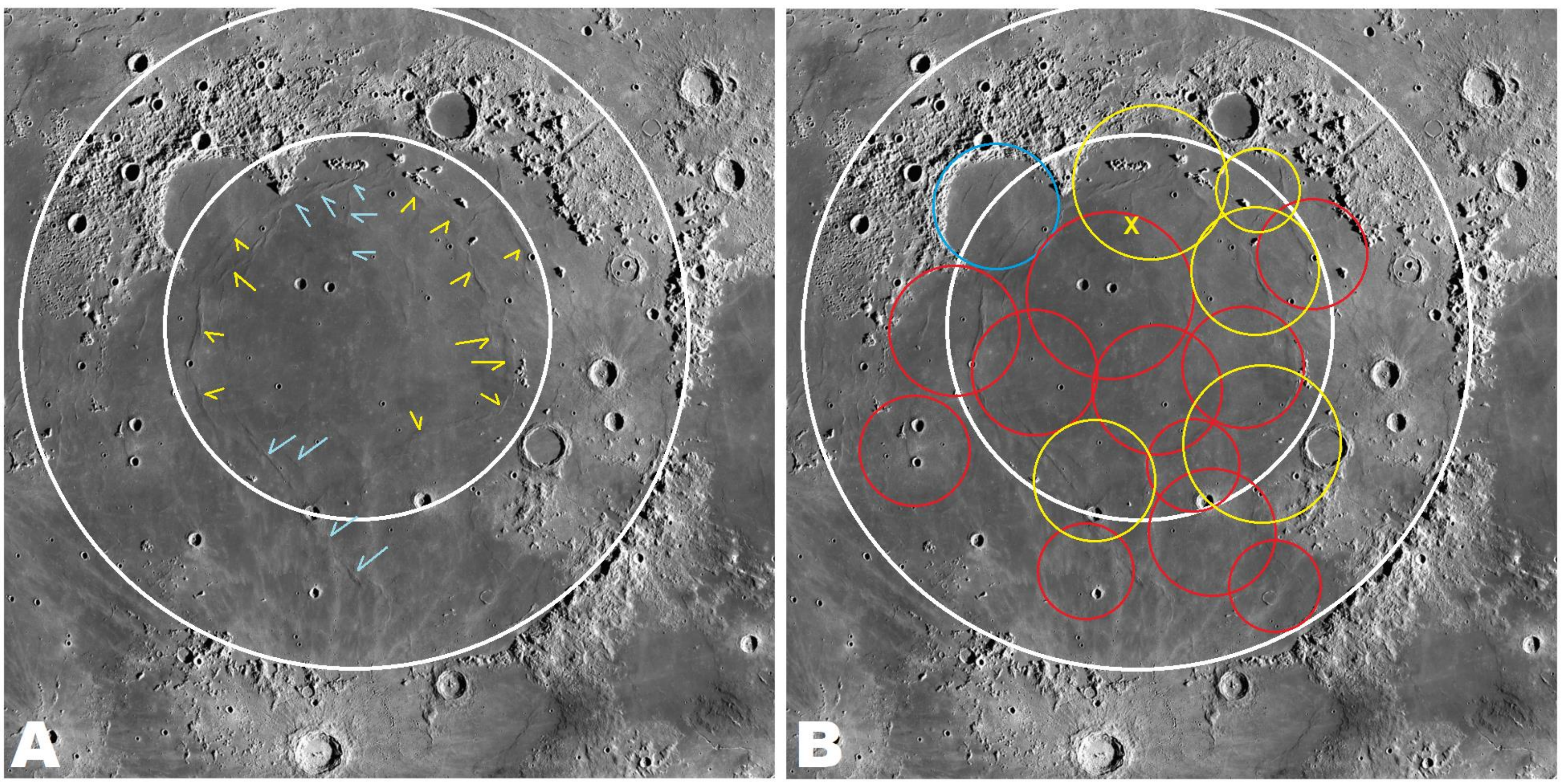

Figure 14.6: Mare Imbrium under ambient light showing the lava field that fills its crater. (A) The ripples in the lava, blue arrows show ripples lying more in lines, while yellow arrows lie more in arcs indicating smaller craters. (B) Sketched circles of smaller craters seen in darker depressions in the lava. Red ones are seen in ambient light and yellow ones are seen in gravity and crustal thickness. Blue circle is Sinus Iridum.

Seeing the blue/low gravity pattern

Based on South Pole-Aitken Basin and Mare Imbrium we will expect to see blue, low gravity, filling the center in early craters which occurred before there were additional energy signatures in the ground, and later ones inside the OCR-ring but outside the Mascons defined by the Open-ring.

On the North American continent seven large craters and one smaller craters define the major geomorphology of the continent. There are 20-30 more smaller but large craters associated with large structures, like the TONCK, Gulf of Mexico, Great Lakes, Mid Continental Rift, Sierra Nevada, etc., etc. which also need to be recognized in the future to fully understand the major geomorphology.

Keys crater (Figure 14.7E)

The Keys crater, at 4,840 km diameter, is the largest crater presently recognized in North America. A clear arc can be seen in the northeast quadrant between ring "A" and the white circle of the Open ring. This dark blue is repeated between the white, Open-ring, and the red OCR-ring, except the dark blue is interrupted by an arc of lighter blue concentric to the Bermuda crater's center. A definite gravity ridge also occurs under "A" in the northeast quadrant, possibly due to interaction with the later Bermuda crater like the concentric expression in the Open-ring.

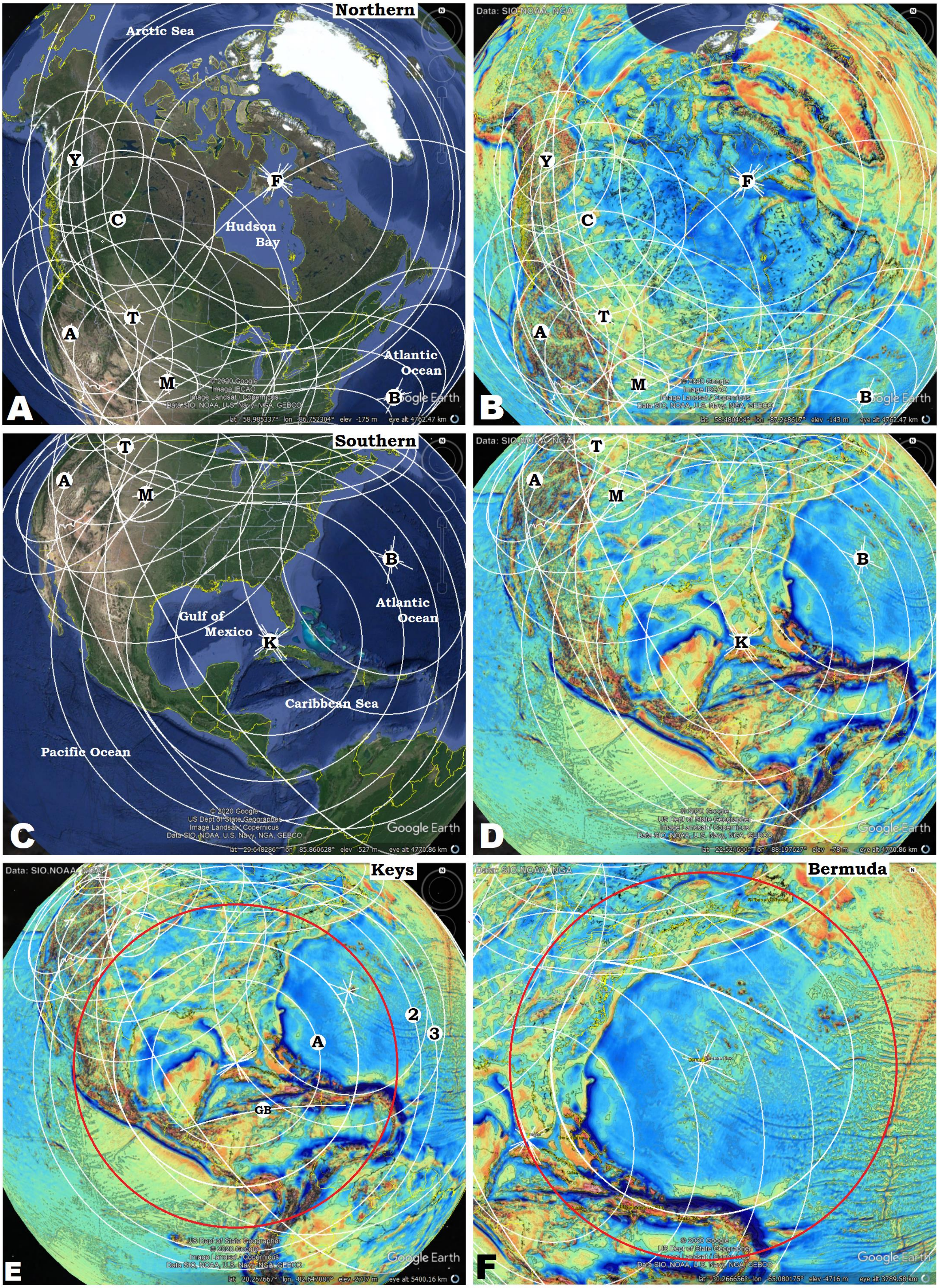
Northern
Arctic Sea
Y
F
C
Hudson Bay
T
A
Atlantic Ocean
M
B
A
Data: SIO, NOAA, NGA
Y
F
C
T
A
M
B
B
Southern
T
A
M
B
Atlantic Ocean
Gulf of Mexico
K
Caribbean Sea
Pacific Ocean
C
Data: SIO, NOAA, NGA
T
A
M
B
K
Google Earth
D
Data: SIO, NOAA, NGA
Keys
2
3
A
GB
Google Earth
E
Data: SIO, NOAA, NGA
Bermuda
Google Earth
F

The Keyes crater can also be seen to ring the yellow-orange area west of Mexico in the Pacific Ocean. Several small blue area in the middle of that area preserves remnants of the release-wave. The 2-ring and 3-ring in the Pacific Ocean suggest an energy stepdown in expression from the OCR-ring.

Additional support for the location of the Keyes' OCR-ring comes from the patches of dark blue against its inside in the due north and northwest portion. The Cayman trench/mascon, marked in white, is a CGRS from the Bahia Grande center just off the west coast of southern Argentina. This suggest that crater may have formed in the same time period as the Keyes crater

Bermuda crater (Figure 14.7F)

The Bermuda crater forms an obvious half circle of blue in the Atlantic Ocean crust and was one of the first large craters identified in gravity by the author. In the east, it warps the highly visible CGRS from the Pacific crater, Chapters 3-5, making it looks like the CGRSs scoop up from the south, or we are looking into a bowl shaped crater. An irregular blue shape parallels the white, Open-ring just beyond it in the southeastern two-thirds of its ocean span.

The southern edge of the Open-ring includes Puerto Rico and the deepest section of the Puerto Rico Trench corresponds to the release wave trough associated with the shock wave ridge. The dark blue of the Puerto Rico trench turns to the south further east and suggest the crater which formed the arc of the Caribbean island also made a large contribution to the energy signature's final expression. The relatively minor portion of the Open-ring occupied by the Puerto Rico Trench and the more pronounced expression of the OCR-ring in the northeastern quadrant determined the designation of each of those rings.

A white arc, mascon trench, extends from the Appalachian Mountains and exits the continent under the Massachusetts peninsula, and continues to the Open-ring. Several chains of small high and low gravity expressions are concentric to the mascon, suggesting it originally involved a larger expression of their interactions. It is a CGRS from one of the impact centers in the Pacific Ocean and occurred in a similar timeframe as the Keys crater.

Looking at the warped linears which seem to form a bowl shape, these lines are CGRS from the Pacific center, Chapters 3-5. I will propose their form is a response to the heated lithosphere when they reached this point, as the shock-release-wave pair would travel through hot rock faster than ambient temperature rock. As the amount of deviation grows greater further to the south, the amount of heating is also increasing showing the interaction of other added impact's heat signature in the lithosphere. Note the Open-ring occurs at the "inside edge' of the "bowl's lip" and the OCR ring occurs at the "outside edge" of the "bowl's edge." This makes the Open-ring and OCR-ring the most important interpretive rings on a crater, and we will refer to them often.

Foxe crater (Figure 14.7G)

The largest blue area of the North American continent, including all of eastern Canada, is in the Fox crater, centered in the Foxe Channel north of Hudson Bay. Greenland, and the higher gravity surrounding it, fills much of the northeast quadrant, but all of the quadrants show mostly blue. The pale blue extends even past the red, OCR ring in many places to the "2" and even "3" ring. The broken blue band running through the center of Greenland inside the high gravity on its east edge is not quickly recognized, but it is symmetrical to the irregular high gravity bordering the broken blue on the western margin of the artic region suggest the location of the OCR ring is correct.

Rings "2" and "3" border on both sides the Mid Atlantic Ridge as it cuts through Iceland, suggesting that ridge has its expression in multiple cratering events. The heavy white line across the Open ring suggest a mascon. The arc of this line is echoed in the high gravity concentric ridge to the northeast. This CGRS has its center in the mid to southern Pacific. As a mascon trench, like the Cayman Trough in the Keys crater, it represents a release valleys, but a single early impactor cannot pull up the high gravity ridges, as will be seen in later cratering, but still shows the lower gravity of the release portion of the wave.

Maka Luta crater (Figure 14.7H)

Pattern for the Maka Luta crater is missing from the eastern two-thirds of the continent, and the A-ring was first recognized where it thrust up the Front Range in Colorado and Wyoming in Figure 14.7A, just south of the "A" in Figure 14.7H. This pronounced arc occur there as a CGRS ("B") from the Bermuda center that contributed to the energy push. For the Bermuda CGRS to provide that energy at the time the A-ring was being expressed, its energy signature would already be in the ground and the timeframe would not be greatly distance from the formation of the Maka Luta crater. The presence of the Bermuda CGRS implies it is a mascon uplifted when the bottom of the crater rebounded inside the Open-ring. The A-ring also contains a chunk of blue just inside the topographic high that almost connects to a significant area of blue inside its north northeast section. Together these blue/low gravity troughs would correspond to the release portion of the A-ring shock wave. The southern half of the Bermuda mascon shows a significant linear of blue on its eastern side, which would correspond also to the shock-release wave pair arriving from the east.

The Open ring for the Maka Luta divides off several blue areas in the Rocky Mountains on its western third. The most dramatic is on a lighter blue ridge across the major blue area of southern Arizona, and links to several high gravity ridges on the eastern half. The OCR-ring corresponds to a ridge of the Coastal Range from Washington State down through mid-California, where it jumps out to follow the continental shelf down into mid-Baja California Peninsula. On the east coast it defines the one of the major backbone ridges of the Appalachian Mountains. The 2-ring defines the eastern continental shelf from New Jersey to South Carolina. This suggest that continental shelves are the edges of the continents and not part of the ocean basins, and that the Maka Luta crater defines the United States' portion of the North American continent.

Tatanka crater (Figure 14.7I)

The Tatanka Open-ring crossing the Rocky Mountains in its southwest quadrant has a significant blue linear inside the ridge, under the line. Both shock ridge and release valley linears cut across the wide blue linear just inside the western edge of the continent. Whether this interaction between Tatanka and Maka Luta represents a latent energy signature or Tatanka over-riding the Maka Luta cannot be determined. On the east, the Open-ring corresponds to the Mid Continental Rift but also cuts off a mascon from the Ipojuca center (I) in the western Atlantic, and I would interpret the Mid Continental Rift as a mascon trough from the combined effort of Maka Luta and the later MAR crater. The Tasman Sea CGRS (TS) forms the major linear of the Rocky Mountains and ends at the Tatanka's Open ring on the south. The northern extension is partly an expression from the Foxe inside its 2-ring added to by the CGRS energy signature from the Tasmanian Sea.

The Tatanka OCR-ring is divided off by some very distinct blue area in the southwest quadrant, both a wide light blue and several spots of dark blue against the OCR-ring. This is repeated on an even larger scale in the northeast quadrant where it crosses the Foxe crater and extends well into the northwest quadrant. Here the OCR-ring lays on a distinct lighter blue ridge in the east and the north and several isolated high gravity spots in between.

Alvord crater (Figure 14.7J)

As a smaller crater, the Alvord was difficult to pick out of several competing circular arcs in the Rocky Mountains. The smaller dark blue arc within its southeast quadrant was especially hard to visually separate. Between that dark blue linear and the Open-ring is a wide dark blue band containing the wiggly thin white line tracing the Colorado River, including the Grand Canyon in its middle third. Many of the Laramide Orogeny arches are also located just outside of this dark blue arc, although some are distributed as far away as the OCR-ring.

The broken blue section of the Maka Luta in Southern California and Northern Baja California was the most distinct indication. That break becomes darker blue towards the south where it follows inside the OCR-ring as a release-wave. It continues east of the Baja California ridge through Arizona. Looking to the north, blue occurs in the same location dividing the British Columbia continental shelf the same way, and extends well inland under the Central Interior Plateau of British Columbia after crossing the Pacific Coast Range.

Caribou crater (Figure 14.7K)

The Caribou crater is not that dissimilar in size to the Alvord, but the Caribou crater defines the east coast of British Columbia, and Alvord has the western third of its perimeter lost in the oceans sea floor. What determines the edges of the continents are not evident at this time, but crater size does not seem to be part of the deciding criteria.

The blue under the Central Interior Plateau of British Columbia extends north and south of the identified portion from the Alvord and lines the Open-ring and extends to valleys east of both ends. The OCR-ring shows the Haida Gwaii islands (1) to be the ridge from a shock-wave and the Hecate Strait (2) that separates them from the mainland and extends past Vancouver Islands well inland showing low gravity from the release valley.

The northeastern half of the Caribou crater is totally lost in the arc of dark blue from the Foxe crater. The smaller size of the Caribou impactor compared to the Foxe impactor suggest the energy envelope from the late Caribou impactor was totally swallowed up in the heat from the first.

The Yukon Gold crater further to the northwest will not be detailed at this time.

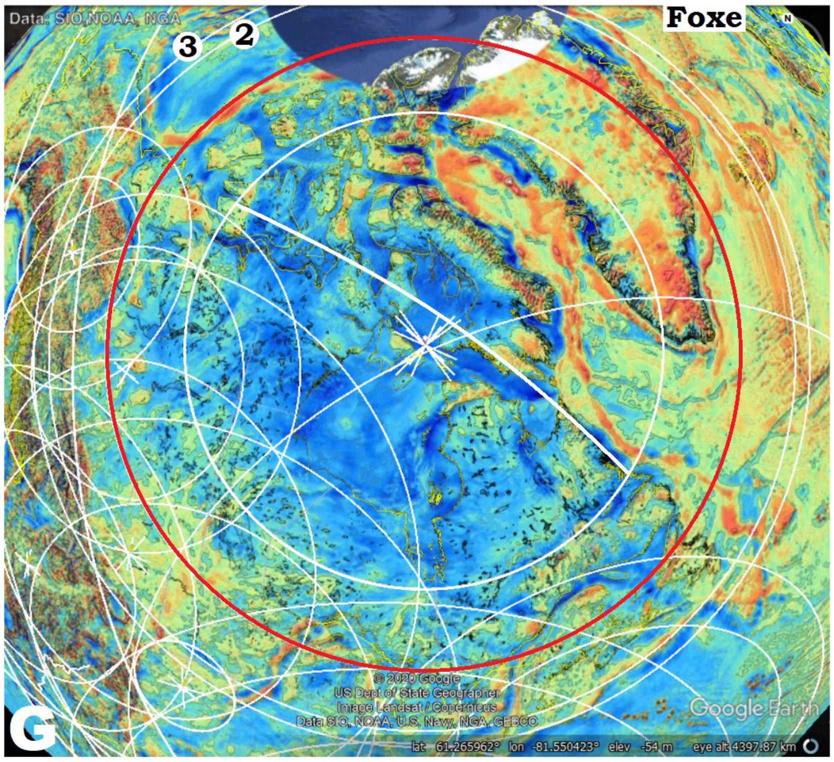

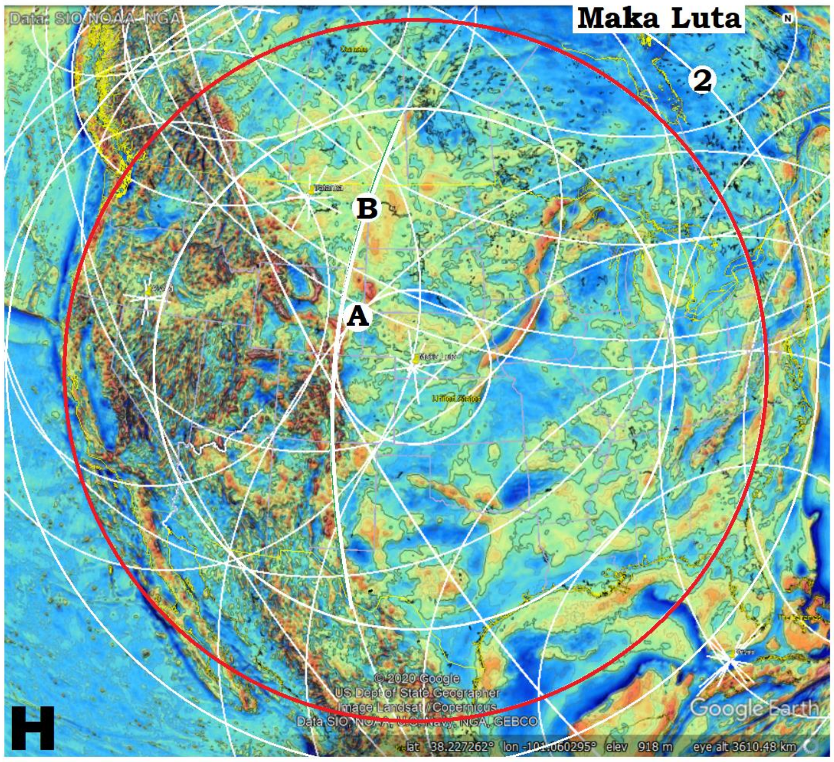

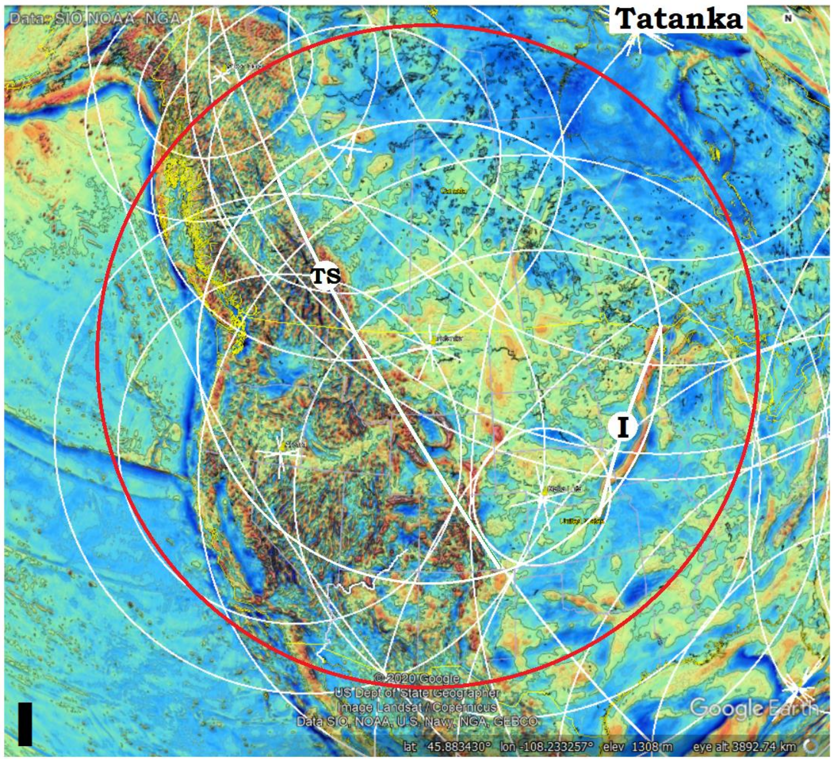

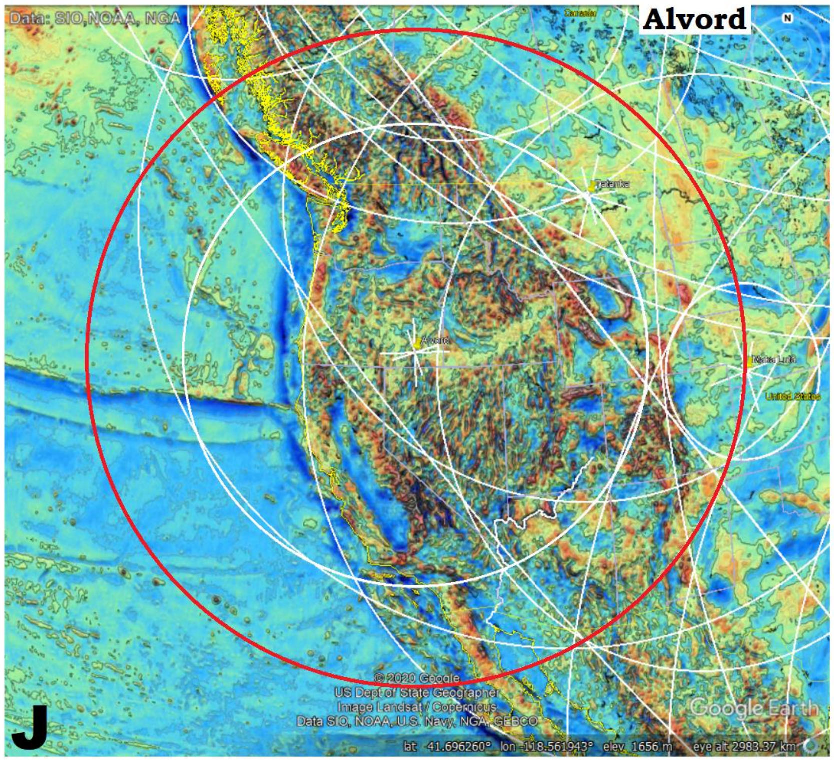

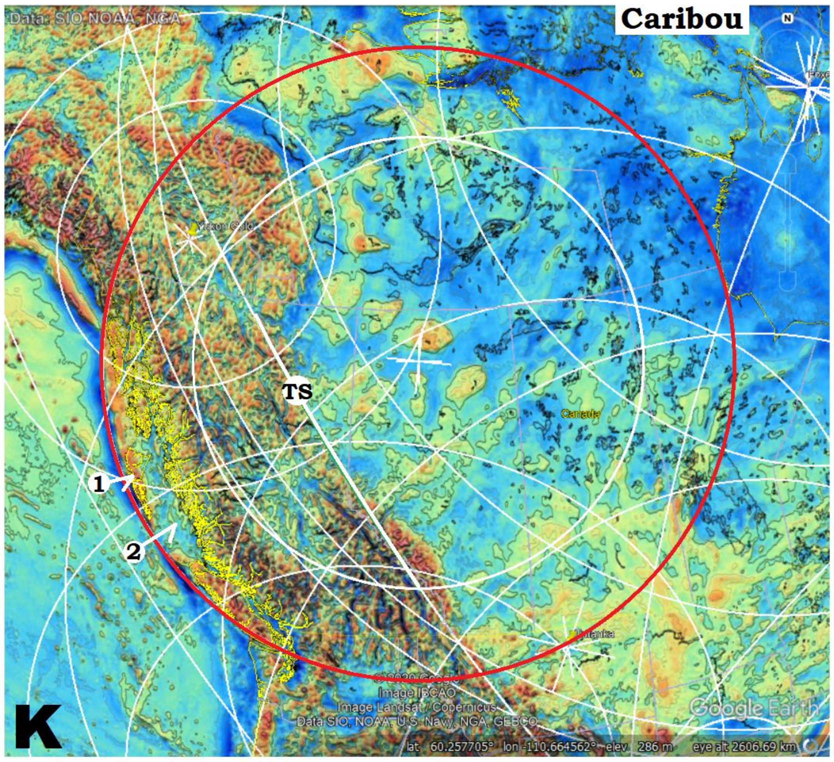

Crater Stats

Crater	Latitude / Longitude	Open Ring Diameter	OCR Ring Diameter	Source of Name
Alvord	42.553612° -118.485099°	2.000 km	2,925 km	Alvord Desert, Oregon
Bermuda	32.165132° -65.644819°	2,960 km	3,890 km	Bermuda Island, Atlantic Ocean
Caribou	58.343084° -115.964586°	1.680 km	2,440 km	Named for the animal
Foxe	64.586369° -80.161244°	3,360 km	4,550 km	Foxe Channel, Luke Foxe explorer 1631
Keys	23.755746° -82.922128°	3,480 km	4,840 km	Florida Keys
Maka Luta	40.541866° -100.931942°	2,750 km	3,900 km	Lakota: Red Dirt
Tatanka	48.278175° -108.311195°	2,700 km	3,900 km	Lakota: Great Beast, Buffalo
Yukon Gold	61.539220° -132.402700°	1,120 km	1,900 km	Yukon route to gold fields

Figure 14.7: Identification of the seven major crater which were probably first to strike the North American continent

Timing and sequence of these craters

Assuming craters arrived from one point in the sky, they would strike the earth from east to west as the planet rotated under the stream of impactors. They would also arrive at roughly 24 hour intervals as a specific spot of the planet's surface rotated into the stream of impactors for about 12 hours and then rotated out of it for about 12 hours. While these large impactors might have been accompanied by a plethora of smaller impactors, the greater energy behind the larger impactors would obliterate any evidence for the smaller ones. This leads to a reasonable assumption, the impactors which left evidence arrived generally in an order of diminishing size. With these four assumptions we can start looking at the larger impactors which might have arrived early in the bombardment of North America.

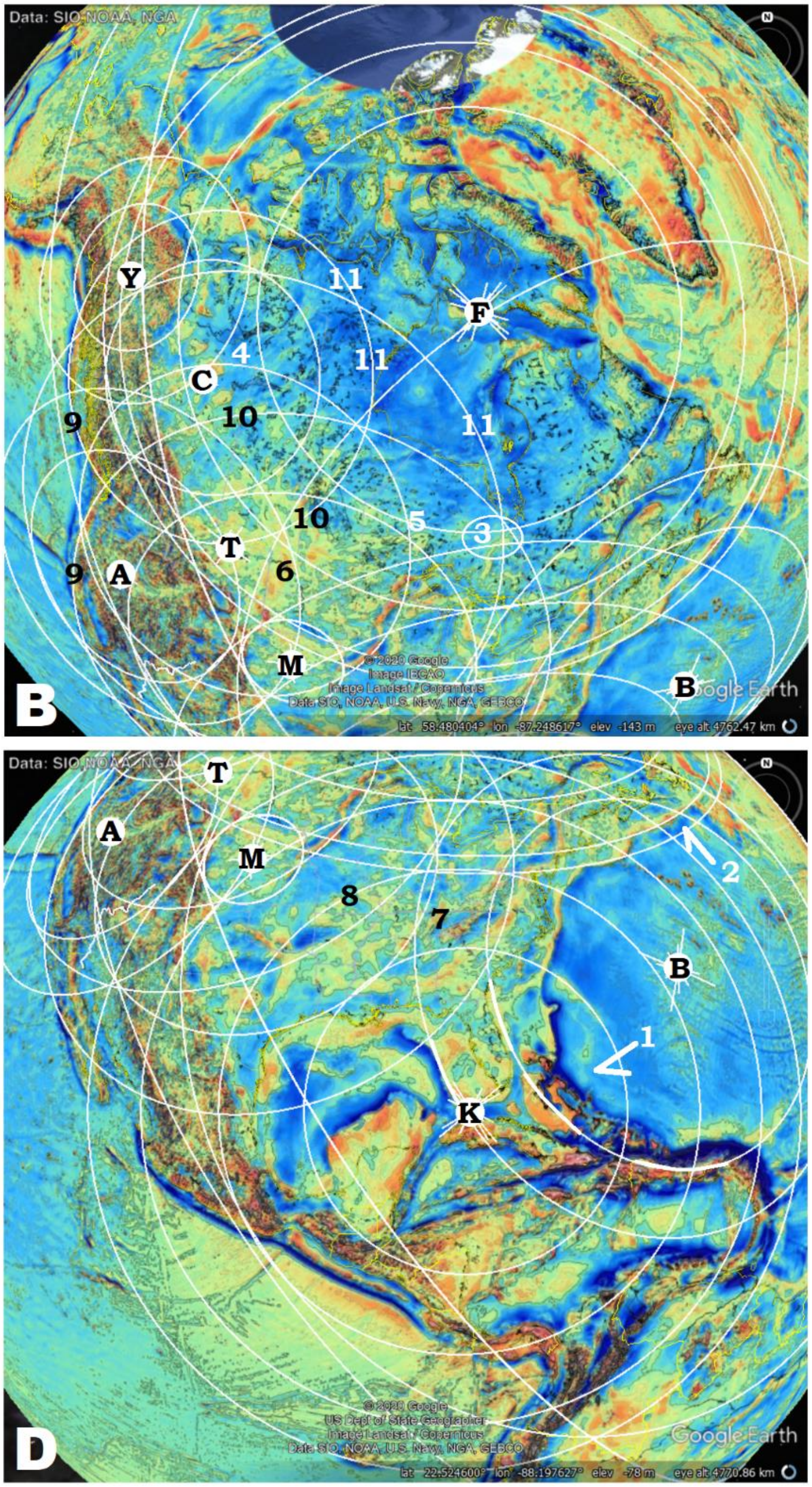

A careful consideration of Figure 14.8 looking for points of interaction of these craters to determine the order. Arrow-1 shows the Bermuda center's gravity changes more prominently and the white arced lines in the Bermuda Open-ring crosses the OCR-ring of the Keyes, the Bermuda crater came after the Keys crater.

On the northwest of the Bermuda crater its underlaps the Foxe crater, arrow-2, while on the southwest it overlaps the Keys crater. If we assume these three impactors were at least one day apart, we have three days of impacts, with the order: 1) Keys, 2) Bermuda, and 3) Foxe.

At point "3" Foxe's pattern also overlays Keys, so Foxe came later. At point "4" Bermuda and Tatanka underlays Caribou. At point "5" Foxe overlays Tatanka and Bermuda. At point "6" Alvord is broken by Foxe and Maka Luta. At point "7" Maka Luta overlays Keys and Bermuda. At point "8" Maka Luta breaks the expression of the Keys but the Keys was probably a larger crater because its energy signature was retained as an upthrust through the pattern of the Maka Luta. At point "9" both Maka Luta and Caribou contributed to the coast line and meets at a perfect V-shape joint. Both overprint the release valley of the Alvord. At point "10" interaction of Caribou and Maka Luta suggest a near simultaneous arrival. At points "11" that pattern of non-interaction is extended to the Foxe.

Figure 14.8: A pattern of overlap by these craters can be recognized at various points.

Two additional relationships of sediments to these craters needs be considered, the pattern of Precambrian sediments and the pattern of mid Cambrian sandstones.

Grand Canyon's Precambrian

The strata of the Grand Canyon is famous among secular geologist as a textbook for the millions and billions of geological age. The lowest sediments in the Unkar Group are dated at 1.84 billion years and the top Kaibab Limestone is dated at 270 million years (National Park Service 2020) which makes the long time scale of millions and billions of years for the earth seem somewhat reasonable. Among Creation geologist the Grand Canyon has also been a favored place for research.

The lowest sedimentary strata, the Unkar group starts with the Bass Formation. The Bass Formation is correlated (Lathrop 2018) with the Middle Crystal Spring formation of the Pahrump Group in Death Valley, the Mescal Limestone of the Apache Group in Central Arizona, the dolomite-bearing units in the lower part of the Debaca Sequence in east-central New Mexico and Texas, and the Allamoore Formation (Van Horn) and Castner Marble in Franklin Mountains of west Texas. His correlations were based on geochronology, lithology, depositional environments and cross-cutting relationship with regionally common mafic dikes. Additionally, he identified two regional fault systems common to these exposures, a southwest to northeast reverse fault, concentric with the Alvord rings and a straight linear set of normal faults northwest to southeast.

The base of the Bass Formation is the Hotauta Conglomerate Member which lies in broad channel forms which were derived from a major breakup to the south and southwest of each deposition site, with conical stromatolite heads among the rubble. Repetition of fine lamina facies indicates a rhythmical wave sourcing of the rubble (Lathrop 2018).

Looking back at the regolith structure of Mare Imbrium (Zhang et al 2019), there were multiple hard layers at 195, 215, and 345 m. Within the top ~14 m which may and probably does represent a much smaller and later crater, four distinct layers of regolith existed. From the bottom, a coarse breccia up to 2.0 m diameter lay on a hard surface, overlaid by a much finer breccia which covered the irregular surface relatively evenly. I will propose it was deposited by settling of aerial particulates. The third layer evened out the surface, starting with settling and progressing to forcibly leveled surfaces, since there is no air to blow on the moon, leveled by the passing of a shockwave. And finally, a pebble surface, where additional force has removed the finer particles.

Lathrop (2018) shows a similar structure in the Hotauta Conglomerate Member at the base of the Bass (his Figure D.21). While only cobble sized clast are pictured, many of them are brick-red or darker on their interior with a whitened surface. I will attributed such changes on the surface to heating and ablation rounding within the adiabatic envelope (Figures 12.7-9). These cobble size breccia are encased in a matrix of smaller breccia, terminating in an irregular surface that turns laminar upwards. Laminar sections end upwards in Mass Flow deposits (his Figure D.22) containing clast of the individual and aggregate lamina. This shows that lithification of laminar elements were almost instantaneous and no time is between laminar and mass flow regimes.

Occurrence of mudcracks in the Hotauta Conglomerate is highly reminiscent of "molar-toothed" structures in the Belt-Purcell Supergroup of British Columbia and Alberta, Canada and Eastern Washington, Idaho, and Montana, U.S.A. except for the missing microsparry calcite infill or replacement. A currently popular hypothesis for formation of molar-toothed structures is the gas expansion and heat stimulated chemical replacement in a gases environment (Kuang 2014). I will propose the sparry calcite replacement in the Belt-Purcell Supergroup was a function of it location much nearer the Tatanka impact location, and the greater heat that would be generated there by contrast to closer to the OCR-ring in the southern deposits. The formation of the various forms of "stromatolites" with their varied forms in several layers of the Unkar could also be explained by some of these same gaseous movements and heat stimulated chemical reactions and precipitations. This would make all stromatolites of a chemical not biological origin and answer many Creationist questions about their occurrence within Flood layers (Wise and Snelling 2005). Stromatolites requires much more study.

The occurrence of the Bass Formation equivalents and the Belt-Purcell supergroup are all contained in the Tatanka crater rings, Figure 14.9.

Above the Unkar Group in the Grand Canyon is the Chuar Group. Beyond the Grand Canyon outcropping, The Chuar is traced northward in Chuar beds drilled for potential hydrocarbons (Lillis 2016), and prominence in the Uinta Mountains (Nagy and Porter 2005). These locations follow the Alvord crater, Figure 14.9.

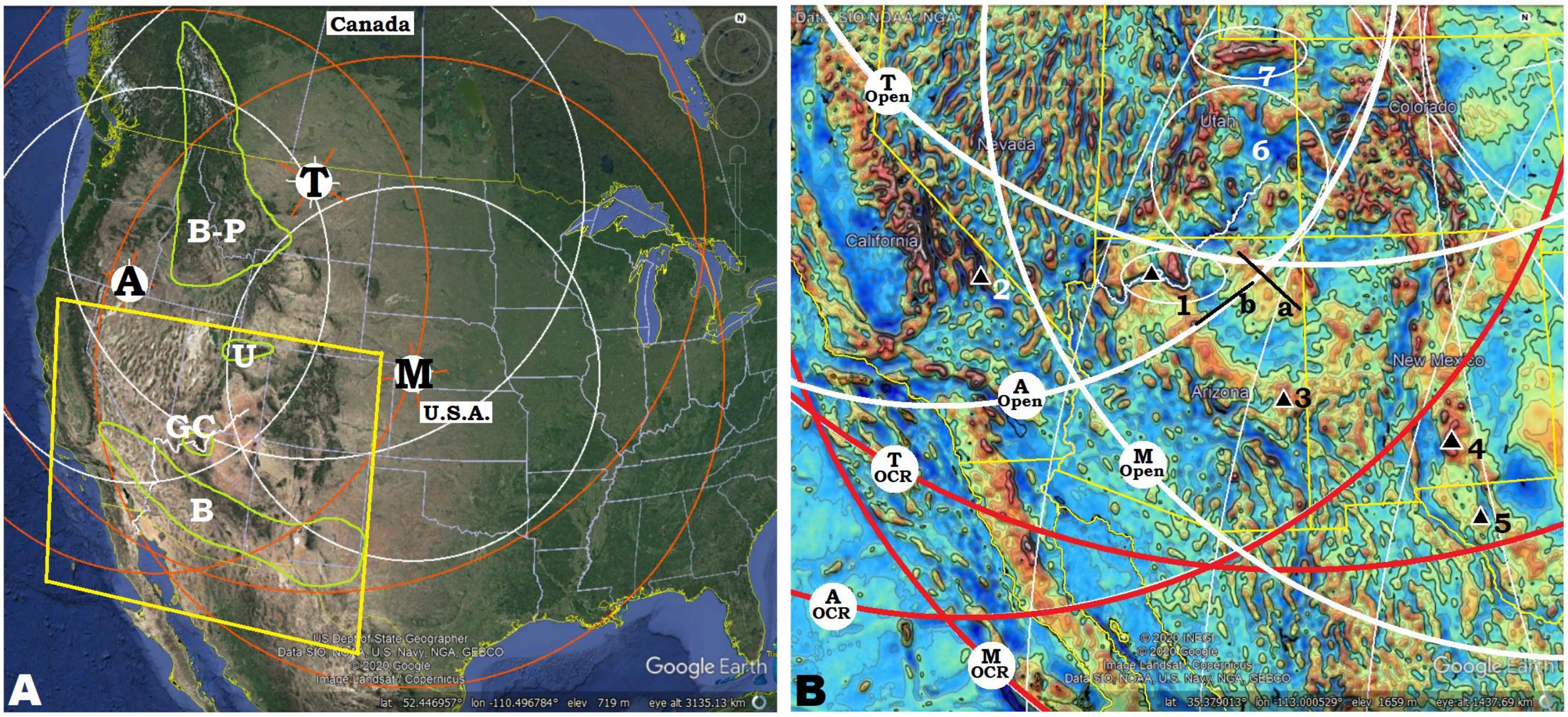

Figure 14.9: (A) Pattern of the Alvord, Maka Luta and Tatanka craters in the North American southwest, and locations of Pre Cambrian strata in that area. Detail of the crossing Locations of Bass Formation 1-5, locations of Chuar Group 1, 6, and 7. Belt-Purcell Supergroup (B-P)

Immediately above the Unkar and Chuar (Precambrian) Supergroups in the Grand Canyon is the Tapeats Sandstone. The Tapeats is the lowest member of the Tonto Group, comprised additionally of the Bright Angel Shale and Muave Limestone. Across Wyoming the Flathead Sandstone, and its equivalent to the southeast, the Deadwood Sandstone occur just above the Great Unconformity. The Flathead Sandstone continue upwards in much of its range with the Gros Ventre Formation, a greenish-gray calcareous shale [similar in color and structure to the Bright Angel shale], and the Gallatin Limestone. This forms a three part formation similarly composed to the Tonto Group of the Grand Canyon.

Sandstones of mid Cambrian age, found just above the Great Unconformity, are often groups as equivalent with the Grand Canyon's Tapeats Sandstone and Flathead Sandstone of Wyoming, including: Tintic quartzite in central Utah, Ladore quartzite in northeast Utah, Sawatch Sandstone of Colorado, Deadwood Quartzite of South Dakota, Lamotte Sandstone in the Ozarks, and Potsdam Sandstone of the Ohio Valley to upstate New York (Hoesch 2007).

Stratigraphic columns across Wyoming shows the occurrence of the Flathead and Deadwood Sandstone, Figure 14.10. Plotting it on the state map by area, the Deadwood Sandstone is shown to approach the plotted A-ring of the Maka Luta crater, but the Gallatin and Gros Ventre remain further away. I would interpret the three layers as originating in vapor condensates from the hot vapor cloud produced by the event, with condensation varying as the vapors cooled (Africano and Bernard 2000, Africano et al 2002, Africano et al 2003). The condensate retained it heat as it neared the hotter area above the impact site, and the nature of the condensate changed from Flathead Sandstone to Deadwood Sandstone. As heat continued to rise above the impact the cooler condensates, shale and limestone, failed to condense there.

These sandstones and more are often grouped in the lowest Sauk group, which is described as the first transgressive sequence. Clarey and Wernerillustrates the occurrence of the Sauk Group in Figure 14.1B. I would explain the large hollow in the Foxe crater from the rebound of the original crater (as in Figure 14.3 section of the South Pole-Aiken crater) and was subsequently eroded off. Alternatively, we do not understand the process for larger craters, and the Foxe center may have exceeded the area of the center of the Maka Luta, as its diameter exceeded the Maka Luta's (almost 20% larger).

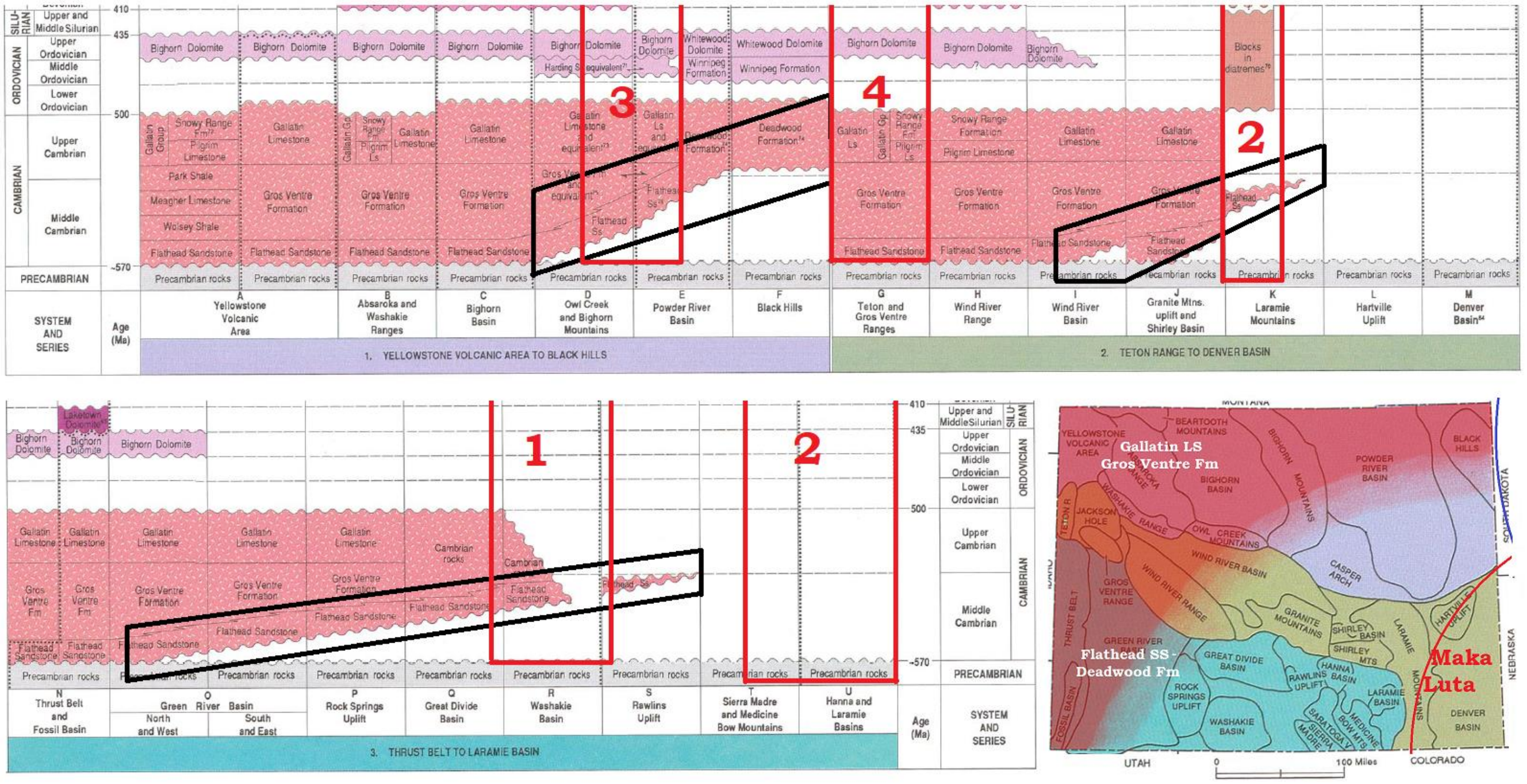

Figure 14.10: Distribution of the Flathead Sandstone and Deadwood Formation across Wyoming and its relationship to A-Ring of the Maka Luta crater. Gallatin Limestone and Gros Ventre Formation are layers above the Flathead Sandstone; all forming a sedimentary unit.

Figure 14.11: (A) The Maka Luta and Foxe craters showing their Open-ring (white) and OCR-ring (red). One CGRS for the Keys crater is shown that corresponds to the “Dinosaur Peninsula” of Clarey. The Sauk Group as portrayed by Clarey showing its correspondence to the crater rings. (B) Redrawn from Clarey and Werner 2017.

Discussion / Conclusion

If topography is the primary form of evidence for interpreting geology (Henry 2009, p 575), understanding the causation behind an expression of energy within that topography is critical to understanding what we see. Since none of us were there to witness the origin, my goal has been to show cratering is just as reasonable an alternative to produce the observed topography, and that it fulfills the evidence seen in gravity maps.

From the overlap of craters and the strata sequence in the Grand Canyon I have plotted the craters to impact in this sequence: Keys crater, 5,035 km diameter, Day 1; Bermuda crater, 3,890 km diameter, Day 2; Tatanka crater, 3,900 km diameter, Day 3, producing the Unkar Supergroup with its vapor condensate; Alvord crater, 2,925 km diameter, Day 3, producing the Chuar Supergroup with its vapor condensate; Foxe crater, 4,550 km diameter, Day 4; contributing to the Sauk basal sandstone; Maka Luta crater, 3,900 km diameter, Day 4, producing the Tapeats Sandstone; Caribou crater, 2,440 km diameter, Day 5 or later.

References

Africano, F. and A. Bernard. 2000. Acid alternation in the fumarolic environment of Usu volcano, Hokkaido, Japan. *Journal of Volcanology and Geothermal Research* 97:475-495.

Africano, F., A. Bernard, and M. Korzhinsky. 2003. High temperature volcanic gas geochemistry (major and minoe elements) at Kudryavy volcano, Iturup Island, Kurilarc, Russia. *Vulcânica* 1:87-94.

Africano, F., G. Van Rompaey, A. Bernard, and F. Le Guern. 2002. Deposition of trace elements from high temperature gases of Satsuma-Iwojima volcano. *Earth Planets Space* 54:275-286.

Clarey, T.L. and D.J. Werner. 2017. The sedimentary record demonstrates minimal flooding of the continents during Sauk deposition. Answers Research Journal 10:271-283.

Goddard Space Center. https://earthsky.org/space/mystery-mass-moon-south-pole-aitken-basin, accessed 11/21/2020.

Henry, C.D. 2009. Uplift of the Sierra Nevada, California. *Geology* 37:575-576.

Hoesch, W.A. 2007. Geological Provincialiam, Acts and Facts, Institute of Creation Research, https://www.icr.org/article/geological-provincialism, accessed 11/28/2020.

James, P., D. Smith, P. Byrne, J. Kendall, H.J. Melosh, and M. Zuber. 2019. Deep Structure of the Lunar South Pole-Aitken Basin. *Geophysical Research Letters.*

Kuang, H-W. 2014. Review of molar tooth structure research. *Journal of Paleogeography* 3(4):359-383.

Lathrop, E.C. 2018. Understanding the Late Mesoproterozoic earth system from the oldest strata in Grand Canyon: C-isotope stratigraphy and facies analysis of the 1254 Ma Bass Formation, Grand Canyon Supergroup, Arizona, U.S.A. Utah State University. *All Graduate Theses and Dissertations.* 7046.

Lillis, P.G. 2016. The Chuar Petroleum System, Arizona and Utah. *Hydrocarbon Source Rocks in Unconventional Plays, Rocky Mountain Region*: 79-136.

Nagy, R.M., and Porter, S.M., 2005. Paleontology of the Neoproterozoic Uinta Mountain Group, in Dehler, C.M., Pederson, J.L., Sprinkel, D.A., and Kowallis, B.J., editors, *Uinta Mountain geology: Utah Geological Association Publication* 33:49-62.

National Park Service. 2020. Age of the Grand Canyon, https://www.nps.gov/articles/age-of-rocks-in-grand-canyon.htm, accessed 11/28/2020.

Wise, K.P. and Snelling, A.A. 2005. A note on the Pre-Flood/Flood boundary in the Grand Canyon. *Origins* 58:7-29.

Zhang, L., Z. Znaofa, J. Li, H. Ling, H. Zhijun, J. Zhang, H. Nan. 2019. A story of regolith told by Lunar Penetrating Radar. *Icarus* 321:148-160.

Zhanga, J., W. Yanga, S. Hua, Y. Lina, G. Fangb, C. Lic, W. Pengd, S. Zhue, Z. Hef, B. Zhoub, H. Ling, J. Yangh, E. Liui, Y. Xua, J. Wangf, Z. Yaoa, Y. Zouc, J. Yanc, and Z. Ouyangj. 2015. Volcanic history of the Imbrium basin: A close-up view from the lunar rover Yutu. *Proceedings of the National Academy of Sciences of U.S.A.* 112(17):5342-5347.